Plant responses to increasing CO_2 reduce estimates of climate impacts on drought severity

Abigail L. S. Swann[a,b,1], Forrest M. Hoffman[c,d], Charles D. Koven[e], and James T. Randerson[f]

[a]Department of Atmospheric Sciences, University of Washington, Seattle, WA 98195; [b]Department of Biology, University of Washington, Seattle, WA 98195; [c]Computer Science & Mathematics Division, Oak Ridge National Laboratory, Oak Ridge, TN 37831; [d]Environmental Sciences Division, Oak Ridge National Laboratory, Oak Ridge, TN 37831; [e]Climate & Ecosystem Sciences Division, Lawrence Berkeley National Laboratory, Berkeley, CA 94720; and [f]Department of Earth System Science, University of California, Irvine, CA 92697

Edited by Christopher B. Field, Carnegie Institution of Washington, Stanford, CA, and approved July 21, 2016 (received for review March 19, 2016)

Rising atmospheric CO_2 will make Earth warmer, and many studies have inferred that this warming will cause droughts to become more widespread and severe. However, rising atmospheric CO_2 also modifies stomatal conductance and plant water use, processes that are often are overlooked in impact analysis. We find that plant physiological responses to CO_2 reduce predictions of future drought stress, and that this reduction is captured by using plant-centric rather than atmosphere-centric metrics from Earth system models (ESMs). The atmosphere-centric Palmer Drought Severity Index predicts future increases in drought stress for more than 70% of global land area. This area drops to 37% with the use of precipitation minus evapotranspiration (P-E), a measure that represents the water flux available to downstream ecosystems and humans. The two metrics yield consistent estimates of increasing stress in regions where precipitation decreases are more robust (southern North America, northeastern South America, and southern Europe). The metrics produce diverging estimates elsewhere, with P-E predicting decreasing stress across temperate Asia and central Africa. The differing sensitivity of drought metrics to radiative and physiological aspects of increasing CO_2 partly explains the divergent estimates of future drought reported in recent studies. Further, use of ESM output in offline models may double-count plant feedbacks on relative humidity and other surface variables, leading to overestimates of future stress. The use of drought metrics that account for the response of plant transpiration to changing CO_2, including direct use of P-E and soil moisture from ESMs, is needed to reduce uncertainties in future assessment.

drought | global warming | climate impact | evaporation | global hydrology

The demand for water by the atmosphere is widely predicted to increase due to climate change (1). It is commonly inferred that this will cause droughts to become more widespread and severe (2). Many recent studies, however, ignore the impact of rising atmospheric CO_2 on plant water use (3–11). Plants absorb CO_2 through stomates in their leaves, and simultaneously lose water to the atmosphere by means of transpiration through the same pathway. Higher atmospheric CO_2 concentrations allow plants to reduce water losses per unit of carbon gain (12), in part by reducing stomatal conductance when the gradient of CO_2 between the atmosphere and the leaf interior increases. If leaf area stays the same, this physiological response has the potential to reduce water losses from the land surface, increase soil moisture, and reduce plant water stress (13)—the opposite effect of an increase in drought stress and aridity as predicted by many drought metrics (3, 14, 15). A plant-centric view may therefore suggest that ecosystem-level tradeoffs between water loss and photosynthesis under increasing CO_2 are potentially large enough to reduce drought, despite the large projected increases in water demand from a warmer atmosphere.

Drought indices, river routing schemes, and water balance models frequently use potential evapotranspiration (PET), rather than actual evapotranspiration, to estimate surface fluxes of water to the atmosphere (Tables S1 and S2). However, even the physically based estimates of this quantity (i.e., the Penman–Monteith equation) do not account for changes in transpiration caused by the physiological response of plants to increasing CO_2, thereby making the implicit assumption that surface conductance is invariant with changing CO_2. Although the climate implications of the physiological effects of CO_2 on plants have been recognized in the literature (16–18), the effects have not been well integrated into studies examining impacts and risks of climate change, including flood risk, water resource stress, predictions of future species distributions, agricultural productivity, and ecosystem processes. Further, the science community uses many different drought metrics (Table S1), and the relative sensitivity of these metrics to plant physiological responses has not been systematically quantified. Our current best estimate of the effects of plant physiology on water fluxes are already integrated within the Earth system models (ESMs) used in the Coupled Model Intercomparison Project, phase 5 (CMIP5), whereby changing atmospheric CO_2 influences transpiration and thus soil moisture. Predictions of available water on land within an ESM are thus disconnected from predictions of drought stress derived from the same model's output using metrics that assume plant and canopy conductance of water remain invariant.

To quantify the effect of increasing CO_2 concentrations on the prediction of drought, we compare idealized experiments for seven ESMs from the CMIP5 archive originally intended to constrain carbon–climate feedbacks, each with a 1% per year increase (from 284 ppm to 1,140 ppm over 140 y) in CO_2 mole fractions, but with the increasing CO_2 influencing different components of the Earth system. We use three experiments to separate the physiological and atmospheric radiative forcing contributions to different hydrologically relevant quantities. One of the three experiments isolates the effect of CO_2 on atmospheric radiative forcing (CO_2rad), so that increases in CO_2 solely influence atmospheric radiative

Significance

We show that the water savings that plants experience under high CO_2 conditions compensate for much of the effect of warmer temperatures, keeping the amount of water on land, on average, higher than we would predict with common drought metrics, and with a different spatial pattern. The implications of plants needing less water under high CO_2 reaches beyond drought prediction to the assessment of climate change impacts on agriculture, water resources, wildfire risk, and vegetation dynamics.

Author contributions: A.L.S.S., F.M.H., C.D.K., and J.T.R. designed research; A.L.S.S. performed research; A.L.S.S. and C.D.K. analyzed data; and A.L.S.S. wrote the paper.

The authors declare no conflict of interest.

This article is a PNAS Direct Submission.

Freely available online through the PNAS open access option.

[1]To whom correspondence should be addressed. Email: aswann@u.washington.edu.

This article contains supporting information online at www.pnas.org/lookup/suppl/doi:10.1073/pnas.1604581113/-/DCSupplemental.

transfer within the ESM. The second experiment isolates the effect of CO_2 on plant physiology (CO_2phys), so that CO_2 directly influences only photosynthetic processes. A third fully coupled experiment combines both effects (FULL) (*Materials and Methods*). We define plant-centric variables or metrics as those that explicitly include the influence of atmospheric CO_2 on plant processes and evapotranspiration. Variables within this class include precipitation minus evapotranspiration (P-E), runoff, and soil moisture. Similarly, we define atmosphere-centric variables and metrics as those that do not allow for surface conductance to change in response to increasing CO_2. Variables within this class include PET and the Palmer Drought Severity Index (PDSI). As commonly formulated, PET is calculated with time-invariant surface conductance (19). Although it is theoretically possible to formulate PET with a sensitivity of conductance to atmospheric CO_2, in practice, this is rarely done because it requires estimating the influence of CO_2 on stomatal conductance, leaf area, and other ecosystem processes. In past work, PDSI has been used as a measure of soil water availability (i.e., refs. 3, 4, and 20) and thus representative of hydrologic drought. We classify it here as atmosphere-centric because PDSI is derived using PET and therefore does not allow for plants to modify surface conductance, yielding a sensitivity to future change driven solely by changing meteorological conditions.

Results and Discussion

All of the models predict increases in PET in the fully coupled simulation both at the global scale (Figs. 1 and 2) and widely across climate space (Fig. 3), with 80% of the change at midlatitudes and lower latitudes attributable to the radiative effects of CO_2 (Fig. 1*A*). The fully coupled response is anticipated from previous work, which shows that increases in PET under future climate change are mainly caused by increases in temperature and vapor pressure deficit (15). Similarly, PDSI, which accounts for both PET and precipitation, decreases in all of the fully coupled simulations in the global average (Fig. 1*E*)—suggesting greater drought stress. Plant physiological responses to CO_2 enhance the contributions from CO_2 radiative forcing by a small amount for PET and by a moderate amount for PDSI, as a consequence of stomatal responses generating a small level of additional warming and contributing substantially to reductions in surface relative humidity (Table S3 and Fig. S1). Drought stress increases for 76% of midlatitude and low-latitude land area when assessed using PDSI.

Using metrics that integrate plant physiological responses to changing CO_2, we find that the pattern of future drought stress is considerably different. All of the fully coupled experiments show an increase in P-E when averaged across midlatitude and low-latitude regions, with the exception of one model that shows little change (Fig. 1*B*). The increases in P-E indicate a reduction in future drought stress, contrasting with the drought response inferred from PDSI. In the fully coupled simulation, 84% of the change in P-E at midlatitudes and lower latitudes is attributable to physiological responses to increasing CO_2 (Fig. 1*A*). We find increases or little change in P-E across most of climate space (Fig. 3*I*). In contrast with PDSI, only 43% of midlatitude and lower-latitude land surface (and 37% globally) has increasing drought stress when assessed using P-E. Continental-scale changes in P-E suggest that drought stress may decrease in many parts of Asia, central and south Africa, Australia, and South America (Fig. 4). This directly contrasts with the predicted response inferred from PDSI and many drought assessments for these regions (e.g., refs. 3 and 4). The two approaches provide

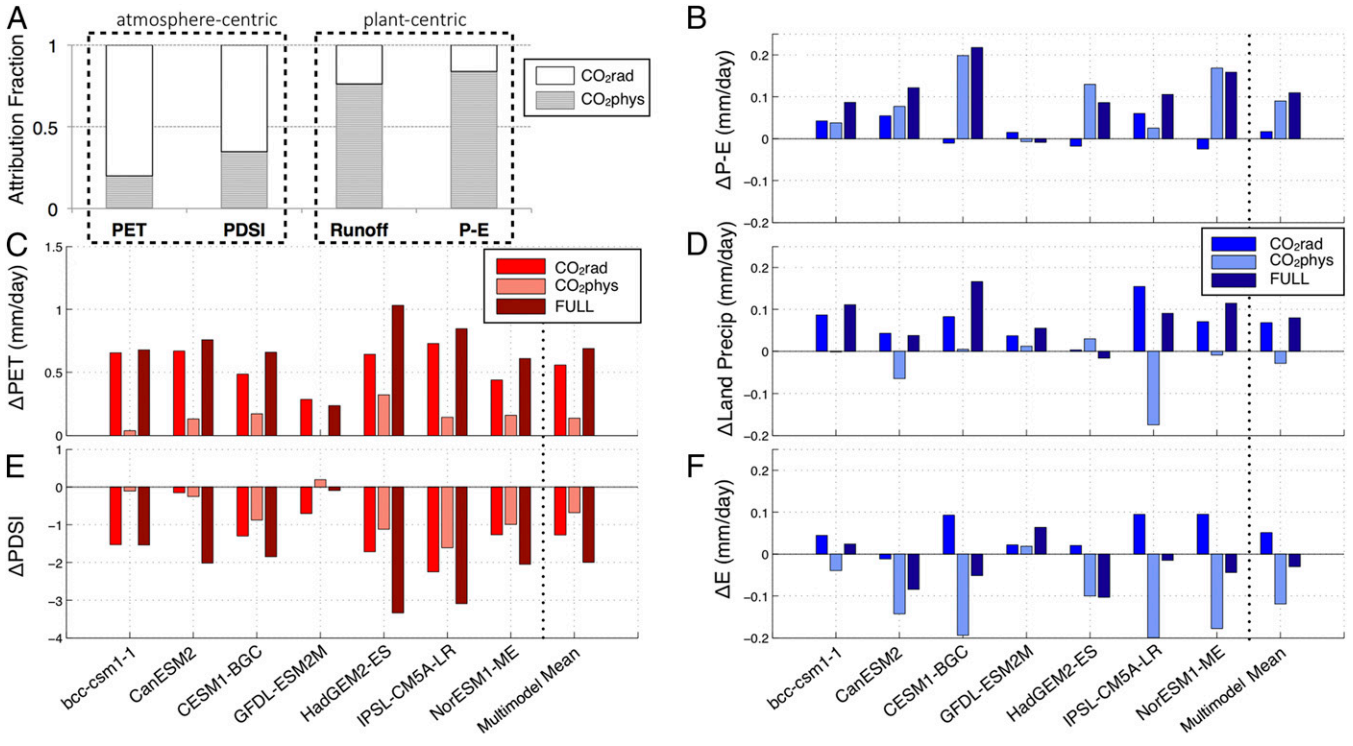

Fig. 1. Midlatitude and low-latitude changes in atmosphere-centric (reds) and plant-centric (blues) metrics and variables, and the attribution of variables to the physiological or radiative effects of CO_2. (*A*) Fraction of the response in the FULL experiment attributable to the CO_2rad (white) and CO_2phys experiments (gray). The difference in the annual mean for latitudes between 45°S and 45°N over a quadrupling of CO_2 is shown for each of three experiments for seven climate models from the CMIP5 archive and the multimodel mean for (*B*) P-E over land (millimeters per day) where larger values indicate more water availability on land, (*C*) PET (millimeters per day) where larger values indicate more water loss from the land, (*D*) P over land (millimeters per day), (*E*) PDSI where larger negative values indicate more severe drought, and (*F*) E (millimeters per day) where positive values indicate a larger flux from the land to the atmosphere.

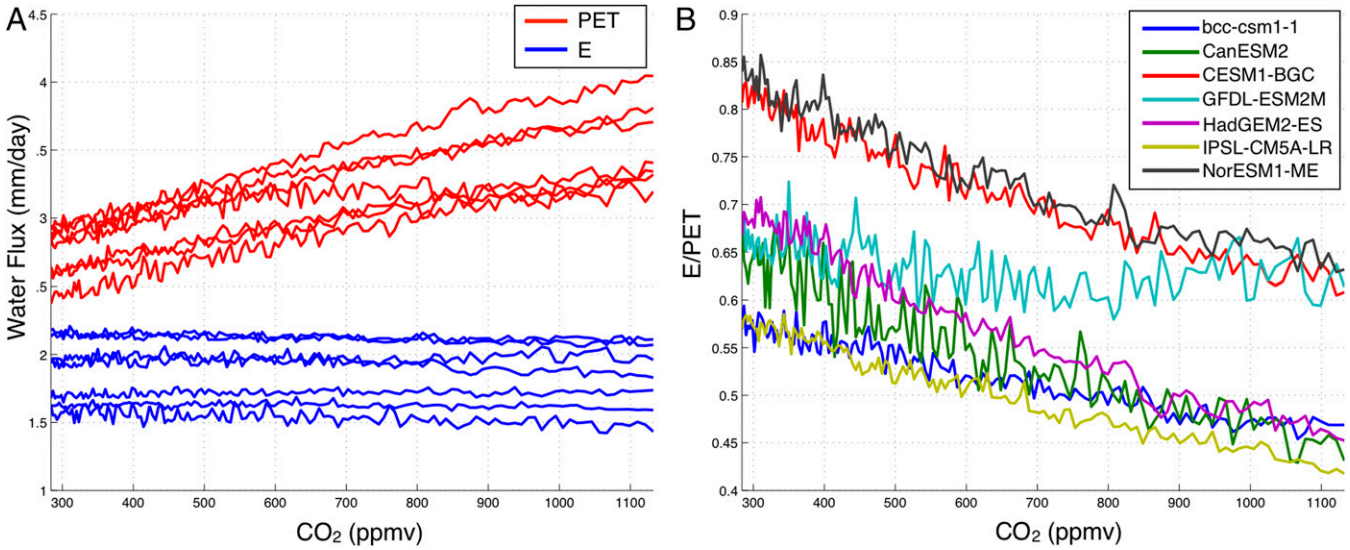

Fig. 2. Time series of (*A*) PET (red lines) and E (blue lines) in millimeters per day for the midlatitude and low-latitude average from each of seven models using the FULL simulation, demonstrating that E remains relatively constant as CO_2 increases despite large increases in PET. (*B*) The ratio between E and PET, averaged over midlatitudes and low latitudes, for each of seven models (identified by color), demonstrating a similar divergence across models between E and PET as CO_2 increases. Note that the GFDL-ESM2M simulation only increases to a doubling of CO_2 (568 ppm by volume), then holds the atmospheric CO_2 concentration fixed; this explains the relatively small changes in E/PET shown during the latter half of the GFDL-ESM2M simulation.

consistent estimates of increasing drought stress in other regions, including southern North America, northeastern South America, and southern Europe (Fig. S2). Higher levels of agreement between the two approaches occur in regions where projected changes in precipitation tend to be more robust (2).

The moderate increase in water available on land, inferred from changes in P-E, is due to both an overall increase in P (Fig. 1*D* and Figs. S2 and S3) and relatively small changes in E (Figs. 1*F* and 2 and Figs. S2 and S3). Precipitation increases in runs with radiatively coupled CO_2 (Fig. 1*D*), as more energy and atmospheric water vapor are available to drive rainfall in a warmer climate (21). Evapotranspiration, by contrast, remains nearly unchanged from the initial values in the multimodel mean, as a consequence of the individual plant physiology and CO_2 radiative forcing drivers inducing large and opposing changes (Fig. 2 and Figs. S2 and S3). Because P and E simultaneously increase in CO_2rad, P-E shows little relative change (Fig. 1*B*). In contrast, E decreases whereas P shows little change in CO_2phys, and thus most of the attribution of P-E change in the fully coupled simulation is to the influence of plant physiology (84%; Fig. 1*A* and Table S3). Modeled changes in soil moisture and runoff are consistent with changes in P-E, albeit with larger intermodel variability owing to significant uncertainty associated with global-scale model representations of these processes (Fig. S4).

Considering only atmosphere-centric drought and aridity metrics (such as PDSI), an approach taken in several recent papers (3, 5–11, 14), the prediction of drought stress in the future is dire. However, studies that use plant-centric metrics (P-E, soil moisture) tend to show a reduced impact (17, 22–25). Our analysis provides a conceptual framework and quantitative approach for reconciling many of these differences; divergence of these two approaches arises primarily from omission or consideration of the physiological effects of CO_2 on plant water needs. Differences in impacts derived from the two types of metrics can be traced to diverging trajectories of PET and E within the models (Fig. 2); PET increases with CO_2, whereas E remains relatively constant because of decreasing levels of canopy conductance. Further, our analysis indicates there is a potential for overestimating drought impacts using metrics derived from ESM model output; PET and PDSI changes are amplified by 19 and 36%, respectively, in the fully coupled simulation because of plant physiology responses to CO_2 (Table S3). Use of these metrics, in turn, in offline analysis to assess crop and physiological drought would double count plant feedbacks on surface humidity, temperature, and net radiation, yielding estimates of future stress that are too high (Table S3 and Fig. S1).

The functional form of stomatal conductance–photosynthesis coupling algorithms integrated within ESMs (26) is generally supported by available observational data (27, 28); nonetheless, the relatively low diversity of representation of this process may contribute to the consistent spatial pattern in E observed across the models. The expected transpiration response of plants to increases in CO_2 remains uncertain, as limited experimental observations of future conditions make it difficult to validate ecosystem-scale behavior of ESMs; however, existing observations tend to show decreases in transpiration and increases in water use efficiency (WUE) with increasing CO_2. The simulations presented here compare moderately well with available field observations (28) (*SI Materials and Methods* and Fig. S5). For six of the seven CO_2 physiology simulations evaluated here, widespread leaf area increases were not enough to offset the influence of decreasing stomatal conductance on E. As a consequence, for this set of models, CO_2-driven growth effects were more than offset by CO_2-driven decreases in transpiration in terms of impacts on the terrestrial water budget. In this context, an important future challenge is to increase the diversity and fidelity of coupling, carbon allocation, and dynamic vegetation algorithms within ESMs, and to develop more effective benchmarking approaches for evaluating these processes. Another important uncertainty is whether individual plant species can tolerate higher levels of atmospheric demand, particularly during seasonal periods of increasingly hot and dry weather (29). For example, intensification of evaporative demand during summers and greater interannual variability in moisture availability may accelerate forest mortality in the western United States (30).

A variety of assumptions are embedded in the choice of metrics used to evaluate the impact of climate change on water resources and land surface processes (Tables S1 and S2). In assessing agricultural drought, for example, it may be appropriate to consider total terrestrial water storage, as human appropriation of water from multiple sources (e.g., from mountain runoff, lakes, aquifers,

and reservoirs) is likely to factor into regional adaptive responses to climate change. Drought-induced tree mortality may be best predicted by soil moisture anomalies, as predawn leaf water potential—which roughly equilibrates with soil water potential overnight—has been shown to be a predictive metric in the southwestern United States (30). In contrast, the appropriate metrics for evaluating fire need to capture the different processes regulating fuel moisture dynamics. Live fuel moisture is sensitive to plant water status and thus root-zone soil moisture, whereas coarse woody debris and surface duff layers may be more sensitive to changes in surface meteorology. Fire weather indices used in climate change studies often rely on atmosphere-centric metrics and variables, and this choice may not adequately capture the response of live fuels or deeper organic duff layers. Further, this study illustrates that relative humidity, a variable known to influence many aspects of fire behavior (31), responds to the influence of atmospheric CO_2 on plant processes by an amount equal to or greater than the radiative effects of CO_2 (Fig. S1 and Table S3). Considering these complexities, we recommend that metrics used to evaluate changes in the hydrological cycle draw upon plant-centric variables from ESMs that already explicitly consider the influence of plants on evapotranspiration, including P-E, soil moisture, runoff, and terrestrial water storage. Advances in measuring soil moisture and total water storage from satellites make these appealing choices for drought assessment (32, 33). By avoiding the use of derived estimates that rely on additional assumptions, it may be possible to reduce uncertainties in impact assessment.

Although the physiological response of plants to increases in CO_2 could be less certain than ESMs suggest, our analysis provides evidence that the current assumption made in many drought prediction studies—that plant water needs will not respond to CO_2—can lead to significant global-scale biases in predicting components of the hydrologic cycle and is not well supported by emerging evidence of increasing plant WUE and decreasing transpiration (34–36). The response of plant water needs to CO_2 is already integrated within ESMs, and thus is already included in analysis of the physical climate reported in the Intergovernmental Panel on Climate Change Fifth Assessment (37). However, inconsistencies arise when an incomplete set of atmospheric and land surface variables from these ESMs is used to construct derived estimates of changing drought stress. Drought metrics such as PDSI have been important tools for assessing the spatial and temporal variability of contemporary drought. As the buildup of atmospheric CO_2 continues to accelerate, however, more sophisticated measures that fully integrate plant and ecosystem responses to the direct effects of changing atmospheric composition are needed to enable policy makers to design effective solutions for managing climate change impacts.

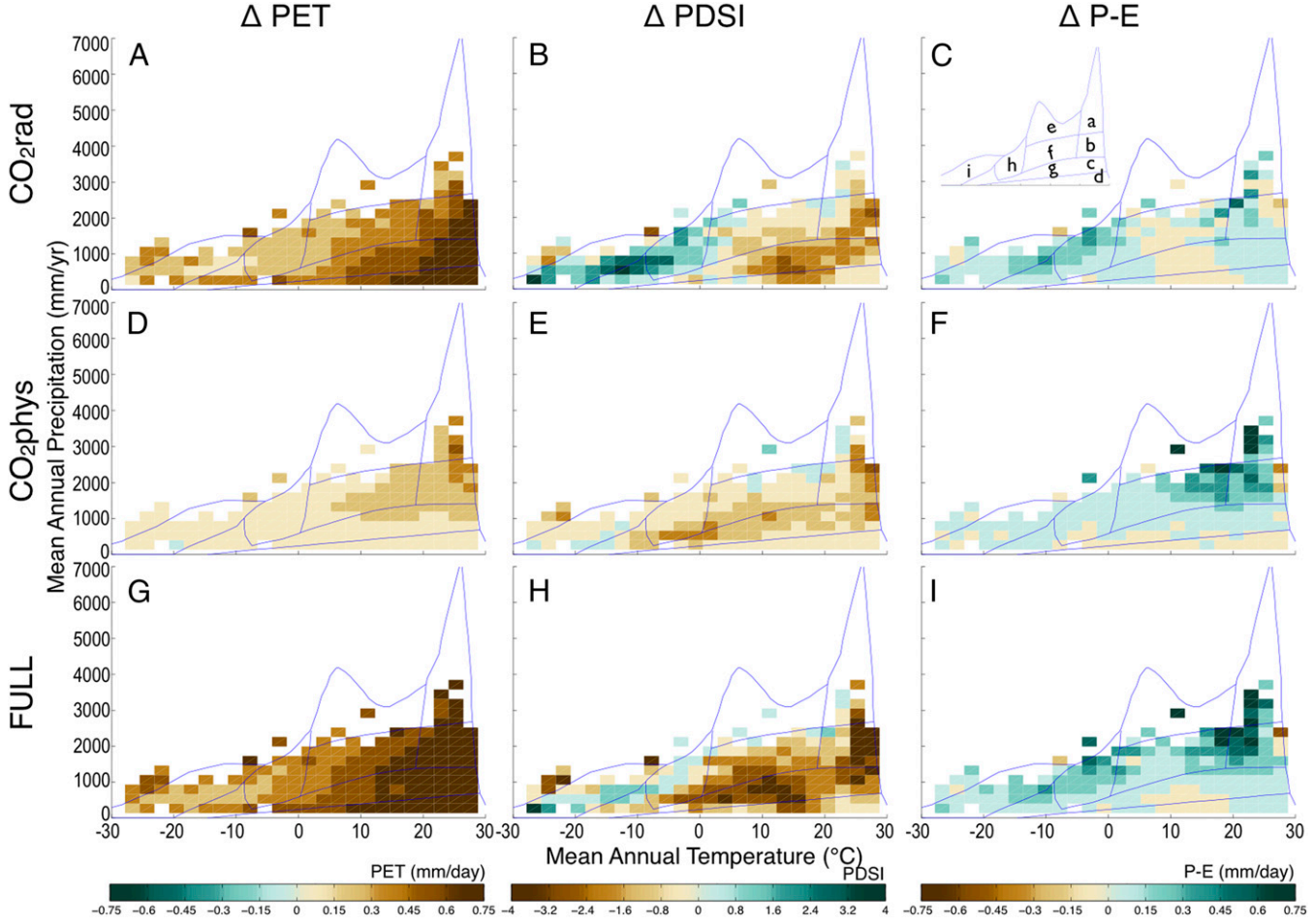

Fig. 3. The change in the multimodel mean of (*A*, *D*, and *G*) PET in millimeters per day, (*B*, *E*, and *H*) PDSI, and (*C*, *F*, and *I*) P-E in millimeters per day for each experiment plotted as the average of all spatial grid points falling at a certain annual average temperature and annual average precipitation. Results are shown for three experiments: (*A*–*C*) CO_2rad, (*D*–*F*) CO_2phys, and (*G*–*I*) FULL. Green colors indicate more water on land, and brown colors indicate less water on land. Blue lines outline biome ranges as reported in ref. 48, shown in *Inset* in *C* identified as: a, tropical wet forest; b, tropical dry forest; c, savanna; d, desert; e, temperate wet forest; f, temperate forest; g, woodland or grassland; h, boreal forest; and i, tundra (see also Fig. S6).

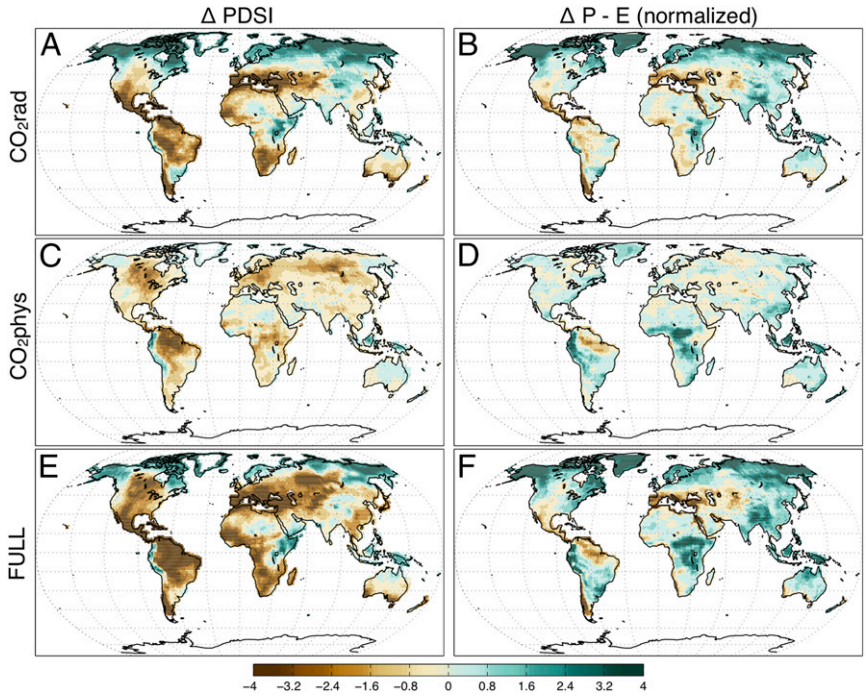

Fig. 4. Maps of the multimodel mean difference over a quadrupling of CO_2 for (*A*, *C*, and *E*) PDSI and (*B*, *D*, and *F*) P-E normalized by the SD of the multimodel mean at each point. Green colors indicate more water on land, and brown colors indicate less water on land. *A* and *B* represent an experiment with only CO_2rad, *C* and *D* represent an experiment with only CO_2phys, and *E* and *F* represent the FULL model.

Materials and Methods

We use the output from seven ESMs (38–44) from the CMIP5 archive (see Table S4) to (*i*) quantify the different continental patterns of drought derived from atmospheric centric and plant-centric metrics and (*ii*) separate the radiative and physiological impacts of increasing CO_2 on different variables and metrics that are widely used in assessments of climate impacts on future drought. These models have full carbon cycles, which include leaf area on land that varies in response to climate and atmospheric CO_2 mole fraction. Two single forcing runs and one fully coupled run were analyzed, each with an idealized 1% per year increase in CO_2 emissions up to a quadrupling of preindustrial atmospheric CO_2 mole fractions, with the exception of the GFDL-ESM2M model (see Table S4 for model information), which increased to a doubling of CO_2 and was held fixed for the remainder of the run (45). In CO_2phys runs (CMIP5 experiment name: esmFixClim1), plant physiology experiences the increase in atmospheric CO_2, whereas the radiation code experiences fixed CO_2. In CO_2rad runs (CMIP5 experiment name: esmFdbk1), the radiation code experiences increasing CO_2 whereas plant physiology does not. The third run analyzed, the FULL run (CMIP5 experiment name: 1pctCO_2), is a combination of the two single forcing runs, where the carbon system is fully coupled, incorporating both effects. Change in a field due to increasing CO_2 is calculated as the difference between the average of the last 20 y with the first 20 y of the simulation. Spatial averages (Fig. 1, Fig. S4, and Table S3) are reported for latitudes between 45°S and 45°N unless otherwise noted. The multimodel mean spatial maps (Fig. 4 and Figs. S1 and S2) were made by first regridding each model's fields to a common 1° × 1° grid, then averaging the different models together.

Seven models were included in this analysis (Table S4). The number of models was limited to those including all variables necessary for the analysis that include near-surface air temperature, near-surface relative humidity, sensible heat flux at the surface, latent heat flux at the surface, precipitation, gross primary production (GPP), and soil moisture. We additionally used the variables for surface winds and runoff where available. A few variables were corrected due to errors in the originally reported data: Relative humidity in the CanESM2 FULL run was adjusted by a factor of 100 and runoff in all runs from IPSL-CM5A-LR were adjusted by a factor of 48 to correct errors noted in the CMIP5 errata (cmip-pcmdi.llnl.gov/cmip5/errata/cmip5errata.html) and bring them into agreement with Earth System Grid Federation standard reporting units.

PET was calculated using the Penman–Monteith approach, as the PDSI has been shown to depend on the choice of formulation of PET (46, 47), and, as in ref. 15, using monthly mean surface values of temperature, latent heat flux, sensible heat flux, relative humidity, and winds. Where wind output was available from the model, it was used; otherwise, winds were held fixed at 1 m/s, as in ref. 3, which found that changes in winds were a minor contributor to future changes in PET. Models where winds were held constant are HadGEM2-ES and NorESM1-ME. PET is calculated using time- and space-invariant surface conductance, as is typical for global studies (e.g., refs. 3, 14, 15, and 19). The PDSI was calculated as in ref. 20 using a MATLAB script from B. Cook but substituting PET that we calculated using a Penman–Monteith algorithm. Values of PDSI larger than 20 or smaller than −20 were discarded as in ref. 3. The baseline period for PDSI was set to the first 20 y of the FULL model run for all experiments in a given model (including CO_2rad and CO_2phys).

The temperature (T) vs. precipitation plots (Fig. 3 and Fig. S3) were made by finding all of the grid cells with annual mean values that fall within each bin defined by bounds in temperature and precipitation and taking an area-weighted average. The multimodel mean of plots in this space was taken by averaging the T vs. P bins together for all models. T vs. P bins are shown only for values of T and P for which at least six models had a value.

The individual effects of radiation and physiology in the FULL experiment are linearly attributed to each of the single forcing components (Fig. 1*A* and Table S3) by calculating the fraction of the FULL run explained by each of the single forcing runs (CO_2phys/FULL, CO_2rad/FULL) and then normalizing by the sum of the total fraction explained by both (CO_2phys/FULL + CO_2rad/FULL). This is equivalent to calculating CO_2phys/(CO_2phys + CO_2rad) as the attribution fraction of CO_2phys and CO_2rad/(CO_2phys + CO_2rad) as the attribution fraction of CO_2rad. The attribution fraction can be larger than 1 if the two single forcing runs have changes of opposite sign. Values of the attribution fraction are plotted for some variables in Fig. 1*A*, and are shown in Table S3.

ACKNOWLEDGMENTS. We thank B. Cook for sharing his software for calculating PDSI and M. Mu for help with retrieving data from the Earth System Grid Federation. A.L.S.S. was supported by National Science Foundation Grants AGS-1321745 and EF-1340649. F.M.H., C.D.K., and J.T.R. received support from the Regional and Global Climate Modeling Program in the Climate and Environmental Sciences Division of the Biological and Environmental Research Program in the US Department of Energy Office of Science. We acknowledge the organizations and groups responsible for CMIP, including the World Climate Research Programme, the climate modeling groups (listed in Table S4), and the US Department of Energy's Program for Climate Model Diagnosis and Intercomparison.

1. Manabe S, Wetherald RT (1975) The effects of doubling the CO_2 concentration on the climate of a general circulation model. *J Atmos Sci* 32:3–15.
2. Collins M, et al. (2013) Long-term climate change: Projections, commitments and irreversibility. *Climate Change 2013: The Physical Science Basis. Contribution of Working Group I to the Fifth Assessment Report of the Intergovernmental Panel on Climate Change*, eds Stocker TF, et al. (Cambridge Univ Press, Cambridge, UK), pp 1029–1136.
3. Cook B, Smerdon J, Seager R, Coats S (2014) Global warming and 21st century drying. *Clim Dyn* 43(9-10):2607–2627.
4. Dai A (2013) Increasing drought under global warming in observations and models. *Nat Clim Change* 3(1):52–58.
5. Sheffield J, Wood EF (2008) Projected changes in drought occurrence under future global warming from multi-model, multi-scenario, IPCC AR4 simulations. *Clim Dyn* 31(1):79–105.
6. Prudhomme C, et al. (2014) Hydrological droughts in the 21st century, hotspots and uncertainties from a global multimodel ensemble experiment. *Proc Natl Acad Sci USA* 111(9):3262–3267.
7. Swain S, Hayhoe K (2014) CMIP5 projected changes in spring and summer drought and wet conditions over North America. *Clim Dyn* 44(9):2737–2750.
8. Asadi Zarch MA, Sivakumar B, Sharma A (2015) Droughts in a warming climate: A global assessment of Standardized precipitation index (SPI) and Reconnaissance drought index (RDI). *J Hydrol (Amst)* 526:183–195.
9. Cook BI, Ault TR, Smerdon JE (2015) Unprecedented 21st century drought risk in the American Southwest and Central Plains. *Sci Adv* 1(1):e1400082.
10. Vicente-Serrano SM, der Schrier G, Beguería S, Azorin-Molina C, Lopez-Moreno J-I (2015) Contribution of precipitation and reference evapotranspiration to drought indices under different climates. *J Hydrol (Amst)* 526:42–54.
11. Zhao T, Dai A (2015) The magnitude and causes of global drought changes in the 21st century under a low-moderate emissions scenario. *J Clim* 28(11):4490–4512.
12. Cowan IR (1977) Stomatal behaviour and environment. *Adv Bot Res* 4:117–228.
13. Field CB, Jackson RB, Mooney HA (1995) Stomatal responses to increased CO_2: implications from the plant to the global scale. *Plant Cell Environ* 18(10):1214–1225.
14. Fu Q, Feng S (2014) Responses of terrestrial aridity to global warming. *J Geophys Res Atmos* 119(13):7863–7875.
15. Scheff J, Frierson DMW (2014) Scaling potential evapotranspiration with greenhouse warming. *J Clim* 27(4):1539–1558.
16. Sellers PJ, et al. (1996) Comparison of radiative and physiological effects of doubled atmospheric CO_2 on climate. *Science* 271(5254):1402–1406.
17. Roderick ML, Greve P, Farquhar GD (2015) On the assessment of aridity with changes in atmospheric CO_2. *Water Resour Res* 51(7):5450–5463.
18. Betts RA, et al. (2007) Projected increase in continental runoff due to plant responses to increasing carbon dioxide. *Nature* 448(7157):1037–1041.
19. Allen RG, Pereira LS, Raes D, Smith M, Ab W (1998) *Crop Evapotranspiration-Guidelines for Computing Crop Water Requirements* (Food Agric Org, Washington, DC), Irrig Drainage Pap 56.
20. Palmer WC (1965) Meteorological Drought (US Dep Commerce, Washington, DC).
21. Pendergrass AG, Hartmann DL (2013) The atmospheric energy constraint on global-mean precipitation change. *J Clim* 27(2):757–768.
22. Orlowsky B, Seneviratne SI (2013) Elusive drought: Uncertainty in observed trends and short- and long-term CMIP5 projections. *Hydrol Earth Syst Sci* 17(5):1765–1781.
23. Koirala S, Hirabayashi Y, Mahendran R, Kanae S (2014) Global assessment of agreement among streamflow projections using CMIP5 model outputs. *Environ Res Lett* 9(6):064017.
24. Chen H, Sun J, Chen X (2014) Projection and uncertainty analysis of global precipitation-related extremes using CMIP5 models. *Int J Climatol* 34(8):2730–2748.
25. Williams IN, Torn MS, Riley WJ, Wehner MF (2014) Impacts of climate extremes on gross primary production under global warming. *Environ Res Lett* 9(9):094011.
26. Collatz GJ, Ball JT, Grivet C, Berry JA (1991) Physiological and environmental regulation of stomatal conductance, photosynthesis and transpiration: A model that includes a laminar boundary layer. *Agric Meteorol* 54(2-4):107–136.
27. Medlyn BE, et al. (2015) Using ecosystem experiments to improve vegetation models. *Nat Clim Change* 5(6):528–534.
28. De Kauwe MG, et al. (2013) Forest water use and water use efficiency at elevated CO_2: A model-data intercomparison at two contrasting temperate forest FACE sites. *Glob Change Biol* 19(6):1759–1779.
29. Allen CD, Breshears DD, McDowell NG (2015) On underestimation of global vulnerability to tree mortality and forest die-off from hotter drought in the Anthropocene. *Ecosphere* 6(8):129.
30. McDowell NG, et al. (2015) Multi-scale predictions of massive conifer mortality due to chronic temperature rise. *Nat Clim Change* 6(3):295–300.
31. Sedano F, Randerson JT (2014) Multi-scale influence of vapor pressure deficit on fire ignition and spread in boreal forest ecosystems. *Biogeosciences* 11(14):3739–3755.
32. Entekhabi D, et al. (2010) The Soil Moisture Active Passive (SMAP) Mission. *Proc IEEE* 98(5):704–716.
33. Landerer FW, Swenson SC (2012) Accuracy of scaled GRACE terrestrial water storage estimates. *Water Resour Res* 48(4):W04531.
34. Peñuelas J, Canadell JG, Ogaya R (2011) Increased water-use efficiency during the 20th century did not translate into enhanced tree growth. *Glob Ecol Biogeogr* 20(4): 597–608.
35. van der Sleen P, et al. (2015) No growth stimulation of tropical trees by 150 years of CO_2 fertilization but water-use efficiency increased. *Nat Geosci* 8(1):24–28.
36. Warren JM, et al. (2011) Ecohydrologic impact of reduced stomatal conductance in forests exposed to elevated CO_2. *Ecohydrology* 4(2):196–210.
37. Stocker TF, et al. (2013) Technical summary. *Climate Change 2013: The Physical Science Basis. Contribution of Working Group I to the Fifth Assessment Report of the Intergovernmental Panel on Climate Change*, eds Stocker TF, et al. (Cambridge Univ Press, Cambridge, UK), pp 33–115.
38. Arora VK, et al. (2011) Carbon emission limits required to satisfy future representative concentration pathways of greenhouse gases. *Geophys Res Lett* 38(5):L05805.
39. Dufresne J-L, et al. (2013) Climate change projections using the IPSL-CM5 Earth System Model: From CMIP3 to CMIP5. *Clim Dyn* 40(9-10):2123–2165.
40. Dunne JP, et al. (2012) GFDL's ESM2 global coupled climate–carbon Earth System Models. Part I: Physical formulation and baseline simulation characteristics. *J Clim* 25(19):6646–6665.
41. Jones CD, et al. (2011) The HadGEM2-ES implementation of CMIP5 centennial simulations. *Geosci Model Dev* 4(3):543–570.
42. Lindsay K, et al. (2014) Preindustrial control and 20th century carbon cycle experiments with the Earth system model CESM1(BGC). *J Clim* 27(24):8981–9005.
43. Tjiputra JF, et al. (2013) Evaluation of the carbon cycle components in the Norwegian Earth System Model (NorESM). *Geosci Model Dev* 6(2):301–325.
44. Wu T, et al. (2013) Global carbon budgets simulated by the Beijing Climate Center Climate System Model for the last century. *J Geophys Res Atmos* 118(10):4326–4347.
45. Taylor KE, Stouffer RJ, Meehl GA (2012) An overview of CMIP5 and the experiment design. *Bull Am Meteorol Soc* 93(4):485–498.
46. Sheffield J, Wood EF, Roderick ML (2012) Little change in global drought over the past 60 years. *Nature* 491(7424):435–438.
47. Hobbins MT, Dai A, Roderick ML, Farquhar GD (2008) Revisiting the parameterization of potential evaporation as a driver of long-term water balance trends. *Geophys Res Lett* 35(12):L12403.
48. Whittaker RH (1975) *Communities and Ecosystems* (MacMillan, New York), pp 111–191.
49. Frank DC, et al. (2015) Water-use efficiency and transpiration across European forests during the Anthropocene. *Nat Clim Change* 5(6):579–583.
50. Schäfer KVR, Oren R, Lai C-T, Katul GG (2002) Hydrologic balance in an intact temperate forest ecosystem under ambient and elevated atmospheric CO_2 concentration. *Glob Change Biol* 8(9):895–911.
51. Wullschleger SD, Gunderson CA, Hanson PJ, Wilson KB, Norby RJ (2002) Sensitivity of stomatal and canopy conductance to elevated CO_2 concentration—Interacting variables and perspectives of scale. *New Phytol* 153(3):485–496.
52. Ainsworth EA, Long SP (2005) What have we learned from 15 years of free-air CO_2 enrichment (FACE)? A meta-analytic review of the responses of photosynthesis, canopy properties and plant production to rising CO_2. *New Phytol* 165(2):351–371.
53. Kolby Smith W, et al. (2016) Large divergence of satellite and Earth system model estimates of global terrestrial CO_2 fertilization. *Nat Clim Change* 6(3):306–310.
54. Dai A (2011) Drought under global warming: A review. *Wiley Interdiscip Rev Clim Chang* 2(1):45–65.
55. Ball JT, Woodrow IE, Berry JA (1987) *Progress in Photosynthesis Research*, ed Biggins J (Martinus Nijhoff, Dordrecht, The Netherlands), pp 221–224.
56. Leuning R (1995) A critical appraisal of a combined stomatal-photosynthesis model for C_3 plants. *Plant Cell Environ* 18(4):339–355.